

RESEARCH ON WHEEL WEAR SIMULATION AND WHEEL-RAIL CONTACT RELATIONSHIP OF HEAVY-HAUL FREIGHT WAGON

Hao Kai¹, Yang Wenkai¹, Zhang Donghui^{1*}, Pei Xinyan², Wang Chen², Xi Yuexiang¹

¹School of Mechanical Engineering, Hebei University of Architecture, Zhangjiakou 075000, China ;

²State Key Laboratory of Mechanical Behavior and System Safety of Traffic Engineering Structures, Shijiazhuang Tiedao University, Shijiazhuang 050043, China

Emails: zdh1304@hebiace.edu.cn

*Corresponding author: Zhang Donghui *

Abstract – In order to study the evolution law of wheel profile wear of heavy-haul freight wagon and the influence of worn wheel profile on wheel-rail contact relationship, taking C80 heavy-haul freight wagon as the research object, the dynamic model of heavy-haul freight wagon and the prediction model of wheel wear were established by UM multi-body dynamics software. Based on vehicle-track coupling dynamics theory, Kik-Piotrowski wheel-rail contact algorithm and Archard wheel wear prediction model, wheel wear simulation research was carried out. Firstly, the correctness of the wheel wear method is verified by measuring the maximum wheel wear, and the wheel wear profile under different mileages is further predicted, and the wear under the wear profile and the variation law of wheel-rail contact parameters are analyzed. The results show that with the increase of running mileage, the wheel wear width increases, and the tread wear width of 1st wheelset is wider than that of 2nd wheelset, and it is close to the root of the wheel. At 70,000 km, the wear width of the 1st wheelset is [- 40 ~ 40 mm], while the 2nd wheelset is [- 40 ~ 36 mm], and the 1st wheelset has serious flange wear, and the flange wear rate of the 1st wheelset is 0.178 mm / 10,000 km higher than that of the 2nd wheelset, and is 2.39 times that of the 2nd wheelset. When the wheel runs up to 50,000 km, the wheel-rail contact point will jump. It is suggested that the wheel flange or rail side should be lubricated when the vehicle runs for 40,000 km in the early stage, and the wheel should be repaired when it runs for 50,000 km in the later stage.

Keywords: Heavy-haul freight wagon; Wheel wear; Wheel parameter; Wheel-rail contact; Equivalent conicity.

1. Introduction

As a pillar of freight transportation, heavy haul railway plays a very important role in the field of railway transportation. The opening of 30,000 tons of train transportation on China 's Daqin heavy haul railway not only marks the goal of railway transportation towards a strong transportation country, but also improves energy emissions such as carbon dioxide to a certain extent [1-2]. As an important part of heavy haul railway transportation, the increasing load and frequent transportation of heavy haul freight wagon will lead to more and more serious wheel wear. The contact relationship between the worn wheel profile and the rail will affect the service life of the wheel and rail [3-5].

In recent years, many researchers have carried out in depth research on wheel-rail contact algorithm and wheel wear prediction. Auciello et al. [6], Meymand et al. [7] and Fang et al. [8] discussed the research of wheel-rail contact dynamics, wheel-

rail contact model and wheel-rail non-Hertzian contact model in multi-body dynamics simulation, and proposed an analytical method for detecting wheel-rail contact points. Roma-no et al. [9] and Marques et al. [10] analyzed the wheel-rail abnormal rolling contact behaviour, and proposed a three-dimensional wheel-rail contact calculation method. Li et al. [11] established a vehicle dynamic model considering wheel wear based on Simpack software, studied the evolution law of wheel wear and dynamic performance of heavy haul freight wagon, and pointed out that the increase of wheel wear will deteriorate the dynamic performance of vehicles. Polach et al. [12-13] demonstrated the behaviour of wheel-rail contact non-linearity at the limit of vehicle stability, and gave the relationship between characteristic parameters and vehicle behaviour. A nonlinear parameter was proposed to evaluate the change of wheel-rail contact point and wheel wear. Aiming at the problems of complex simulation setting, low computational efficiency and insufficient calculation accuracy of wheel-rail contact algorithm

in dynamics, Liu et al. [14-15] proposed a non-Hertzian contact model and a modeling method of conformal wheel-rail rolling contact. Burgelman et al. [16] created a wheel-rail contact model considering creep force based on MATLAB software. Hao et al. [17-18] used the trace method to study the variation law of equivalent conicity between wheel profile evolution and turnout profile, and analyzed the influence of worn wheel profile on the position of wheel-rail contact point. Aiming at the problem of wheel wear prediction modeling, Butini et al. [19] developed a modeling method considering wheel-rail wear and rolling contact fatigue prediction. Wang et al. [20] established a wheel wear prediction model considering the interaction between abrasive block and wheel. Jin et al. [21] studied the wear behaviour between the flange and the gauge angle based on the double-disk tester, and established a predictive wear model considering the wheel-rail contact stress. Based on the finite element model of wheel and rail, Miao et al. [22] and Kaiser et al. [23] studied the influence of flexible wheel structure on wheel wear prediction and wheel-rail contact parameters respectively. Based on the neural network model in machine learning, Singh et al. [24], Shebani et al. [25] and Pires et al. [26] predicted the changes of wheel-rail contact parameters, wheel wear and wheel-rail force respectively. Gao et al. [27], Molatefi et al. [28] and Pacheco et al. [29] optimized the wheel profile. The optimized wheel profile can improve the wheel wear performance, reduce the wear index and reduce the maintenance cost.

The above research has carried out a lot of work on the wheel wear problem of heavy-haul freight wagon from different angles, revealed the evolution law and dynamic correspondence of wheel wear, and also proposed corresponding solutions. However, the research on the matching characteristics of wheel wear profile and rail and the wheel-rail contact relationship of heavy-haul freight wagon has not been deepened. In view of this, this paper establishes the dynamic model of C80 heavy-haul freight wagon, carries out the simulation research of wheel wear, and analyzes the wheel-rail contact relationship of wheel profile after wear, and discusses the evolution of wheel wear and the change law of wheel-rail matching characteristics, so as to provide reference for mastering the evolution law of wheel wear and the optimization of wheel-rail profile of heavy-haul freight wagon.

2. Heavy-Haul Freight Wagon Dynamics Model

2.1 Freight Wagon Model and Line Condition Setting

Based on the basic parameters of the freight wagon dynamics model Table 1 and the multi-body

dynamics theory, the heavy-haul freight wagon dynamics model is established in the UM software as shown in Figure 1. The C80 freight wagon adopts a three-piece bogie, including two side frames, one bolster, four wedges, two cross support rods and other components. The bogie and the car body are mainly connected by the center plate, and the contact force element is used for dynamic modeling. Elastic side bearings are installed at both ends of the bolster to suppress the hunting motion of the bogie. The bolster and the side frame are connected by a spring device and a friction wedge damping device, with a total of 162 degrees of freedom [30-31].

Table 1. The related information of heavy-haul freight wagon dynamics model

Parameter	Value	Unit
Axle load	25	t
Mass,Car body	90.297	t
Mass,bogie	4.8	t
Mass,wheelset	1.171	t
Bogie wheelbase	1.83	m
Vehicle distance	8.2	m
2ndary suspension transverse span	1.98	m
Rolling radius	420	mm
Distance between backs of wheel	1353	mm
Profile of wheel	LM	—
Track gauge	1435	mm
Profile of rail	75	kg/m

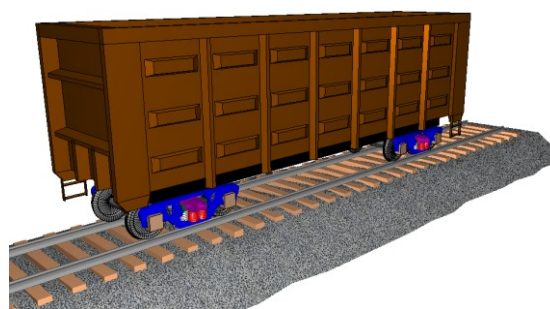


Figure 1: Truck-track coupling dynamics model

As shown in Figure 2, the track uses a moving mass rail model. The model adds a moving mass block under each wheel, which has equivalent mass and rotational inertia, and considers three degrees of freedom of the rail Y, Z direction translation and X direction rotation [32-34]. The transverse force F_{NY} and the vertical force F_{NZ} between the rail and the ground are shown below.

$$F_{NY} = -K_{1Y}(\Delta Y_1 - \Delta Y_2) - C_{1Y}(\Delta \dot{Y}_1 - \Delta \dot{Y}_2) \quad (1)$$

$$F_{NZ} = -K_{1Z}(\Delta Z_1 - \Delta Z_2) - C_{1Z}(\dot{\Delta Z}_1 - \dot{\Delta Z}_2) \quad (2)$$

In the formula, K_{1Y} , K_{1Z} , C_{1Y} , C_{1Z} , ΔY_1 , ΔZ_1 are the lateral and vertical stiffness coefficient, damping coefficient and rail deflection of the rail, respectively. K_{2Y} , K_{2Z} , C_{2Y} , C_{2Z} , ΔY_2 , ΔZ_2 are the lateral and vertical stiffness coefficient, damping coefficient and rail deflection of the sleeper, respectively.

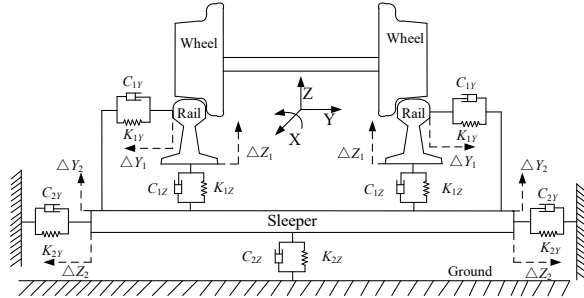


Figure 2: Moving mass rail dynamics model

The Da-Qin Railway is the first double-track electrified heavy-haul coal transportation line in China. It starts from Datong in Shanxi Province in the west and ends in Qinhuangdao in Hebei Province in the east. It is the main channel for 'west-east coal transportation'. The total length of the line is 653 km, and the straight line accounts for 77.71%, of which the 800 m curve radius accounts for 12.48%. In this paper, based on the route distribution and driving speed statistics of Daqin line, the simulation conditions are set as shown in figure 3 [35]. The track excitation represents the track geometrical states of the existing lines, and the China Main Line irregularity spectrum is selected [36]. The horizontal and vertical amplitudes fluctuate within ± 8 mm, as shown in Figure 4 below.

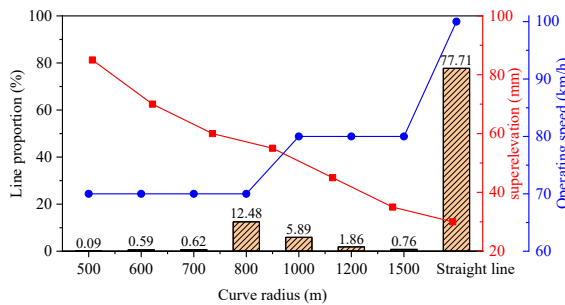


Figure 3: Line simulation conditions and driving speed

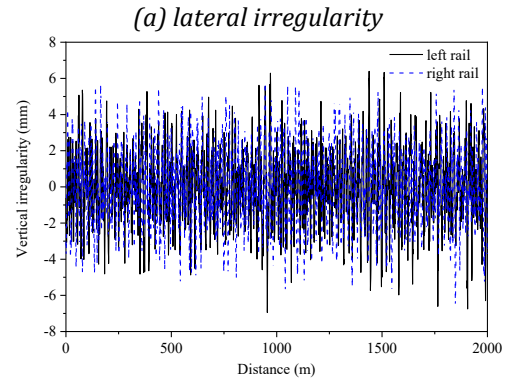
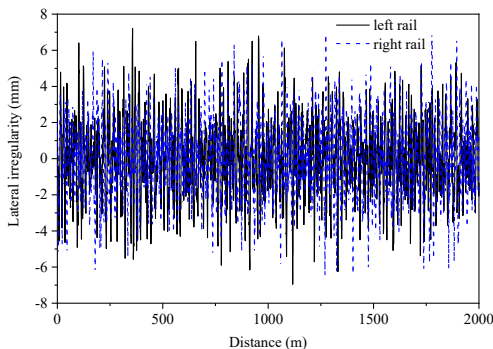


Figure 4: Example of China main line irregularities

2.2 Wheel Wear Prediction Model

For the prediction of wheel wear, it is necessary to further determine the internal relationship between wear and wheel-rail contact force. Archard model is the most mature method [37]. The model assumes a linear relationship between wheel wear volume and wear work [38]:

$$W = k_v A \quad (3)$$

$$k_v = \frac{k_m}{\rho} \cdot 10^{-6} \quad (4)$$

In the formula, W is the volume of wear [m^3], A is the wear work [J], k_v is the volume wear coefficient [m^3 / J], k_m is the mass wear coefficient [mg / J], ρ is the material density, and the mass wear coefficient [39-40] is selected as shown in Figure 5 below.

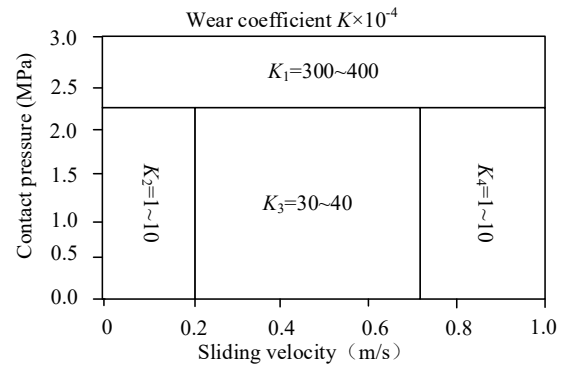


Figure 5: Wear map of the Archard model

By introducing the relationship between wear work and normal force, sliding distance, etc., it can be obtained [41]:

$$W = k_v \frac{Ns}{H} \quad (5)$$

In the formula, N is the normal force, s is the sliding distance, and H is the hardness.

Within a time, integration step Δt , the formula for calculating the wear volume of each contact element in the wheel-rail contact patch is:

$$W_{ij} = k_v \frac{p_{nij} \Delta F_{ij}}{H} |w_{ij}| \Delta x_j \quad (6)$$

In the formula, p_{nij} is the normal stress in the contact element, ΔF_{ij} is the area of the contact element, w_{ij} is the center creep rate of the contact element, and Δx_j is the length of the contact element along the X axis.

Finally, the wear volume corresponding to each unit in the contact spot is accumulated and summed to obtain the total wear volume of the entire contact spot.

2.3 Methods of Wheel Wear

The track length of the discrete vehicle in the simulation process is divided into a series of wear steps. At the end of each wear step, the wear depth is scaled according to the mileage assigned to the wear step to enlarge the wear. The scaling is based on the fact that the small amount of material removed by wear is almost linear, and the amount of wear depends on the distance travelled by the vehicle [42]. The scaling factor formula is as follows:

$$c = \frac{N_{ws} km_{step}}{S_i - S_{bi}} \quad (7)$$

In the formula, c is the scale factor, N_{ws} is the wear step, which is the number of contour updates in an iteration, km_{step} is the mileage allocated to the wear step, S_i is the track length of the rail vehicle during the simulation, and S_{bi} is the track distance at the beginning of the wear calculation.

The wheel wear process is shown in Figure 6. The dynamic data are input to establish the dynamic model of heavy-haul freight wagon and the moving mass rail model. The weight factors of vehicle running speed and track line conditions are introduced to set the weight factors. The specific parameters are shown in Figure 3 above. The initial wheel profile of the freight wagon is LM profile (see Figure 6 of the wheel profile coordinate system, the coordinate origin is the nominal rolling circle contact point of the wheel profile, corresponding to the midpoint of the abscissa profile, the abscissa axis y is parallel to the wheelset axis and points to the flange, and the Z axis is vertical). The wheel-rail contact parameters are calculated by Kik-Piotrowski, and the cumulative tangential creep rate of the wheel is obtained. Then, according to the Archard wheel wear model, the cumulative wear depth is calculated. The wheel profile is updated and returned to the initial wheel profile to complete the iterative calculation of wheel profile wear simulation. The rail base slope is 1/40. In order to improve the computational efficiency and reduce the amount of simulation calculation, it is assumed that the front and rear bogies are symmetrical and the left and right wheels are symmetrical.

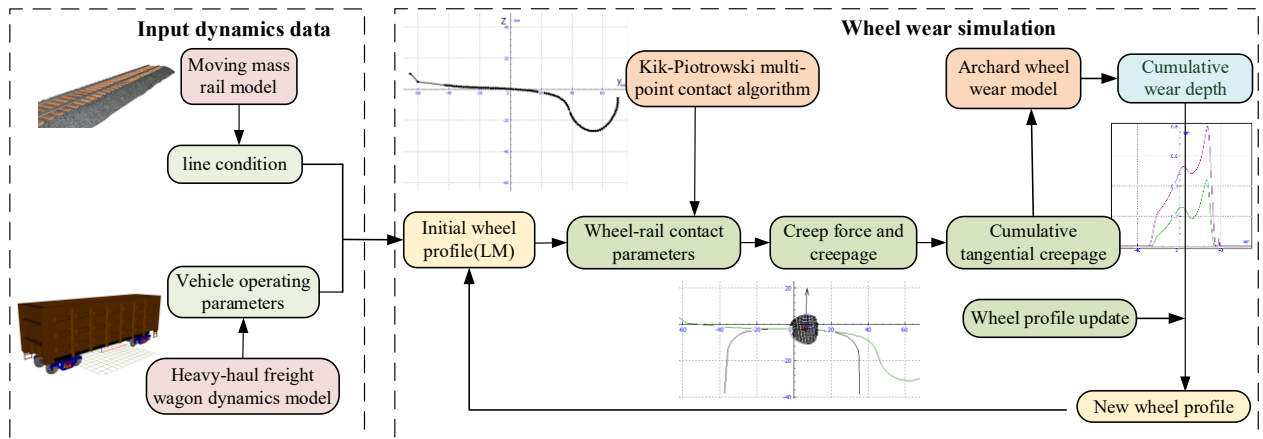


Figure 6: The technique diagram of wheel wear

3. Wheel Wear Simulation Results

3.1 Wheel Wear Method Verification

Based on the measured maximum wear depth data of the wheel, the simulation results are compared. In the wheel wear simulation, 5,000 km is used as the iterative running mileage, with a total of 7 iterations, and the maximum running mileage is 35,000 km. Due to the large number of measured

data and the large difference in some data changes, the measured data are interpolated and fitted by the cubic spline linear interpolation method, and the error value between the measured data and the simulation data is calculated.

Figure 7 (a) shows the comparison between the simulation and the measured results of the 1st wheelset. When the running mileage is 0 ~ 20,000 km, the maximum wear depth of the simulated wheel is lower than the measured result. When the running

mileage is 15,000 km, the maximum error is 0.113 mm. When the running mileage is 20,000 ~ 35,000 km, the overall simulation results are in good agreement with the measured results. When the running mileage is 35,000 km, the minimum error is 0.002 mm. Because the 1st wheelset is the guide wheelset, the wheel wear is relatively bad in the early stage of operation, so the simulation results may be lower than the measured results. It can be seen from Figure 7 (b) that the maximum error of the 2nd wheelset is 0.217 mm at 10,000 km, and the simulation results are very close to the measured results at 25,000 km to 35,000 km. In summary, the simulation data and the measured data are roughly linearly increasing, and the error value is relatively small, which meets the requirements of the subsequent wheel wear simulation.

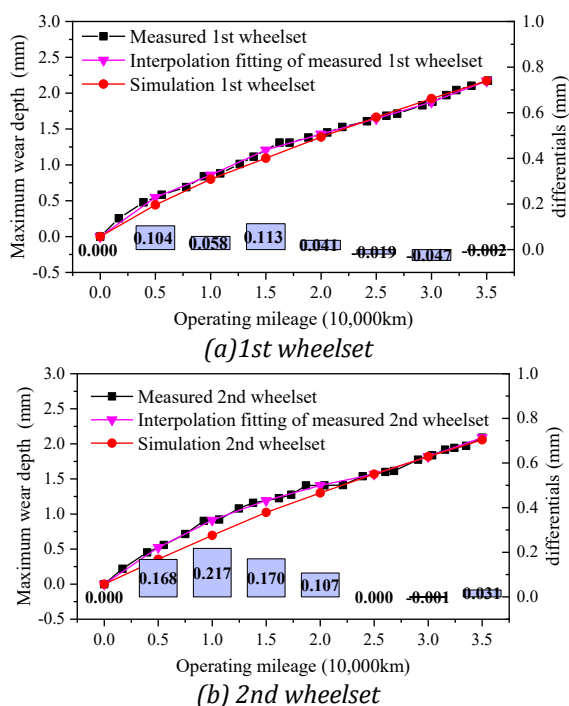


Figure 7: Comparison of measured data and simulation

3.2 Wheel Profile and Wear Amount

Based on the above wheel wear simulation method, the wheel wear simulation iterative running mileage is set to be 10,000 km, and the wheel wear simulation profile and wear amount of 70,000 km are obtained as shown in Figure 8. With the increase of vehicle running mileage, the width of wheel wear becomes larger. When the 1st and 2nd wheelsets are at 10,000 km, the width of wheel wear is distributed between [-30 ~ 35 mm] and [-30 ~ 30 mm]. At 70,000 km, the width of 1st and 2nd wheelsets is distributed between [-40 ~ 40 mm] and [-40 ~ 36 mm]. As the running mileage of the vehicle increases, the wear of the 1st and 2nd wheelsets moves relatively large to the end of the wheel, moving about

10 mm, and moving about 5 mm to the root of the wheel.

Due to the effect of the wheel flange, the wheel-rail contact point moves more widely to the end, and the uniform wear is at the tread [-40 ~ -30 mm] position, while the wheel-rail contact point range is relatively concentrated at the flange position, and the wear amount increases at the [30 ~ 35 mm] position, resulting in serious wear at the flange position.

In the early stage of vehicle operation, when the vehicle is 0 ~ 40 000 km, the wheel wear increases greatly, and then changes slowly, among which the wear at the flange [20 ~ 40 mm] position is the largest. The wear of the 1st wheelset is closer to the flange root than that of the 2nd wheelset, and the wear is higher than that of the 2nd wheelset.

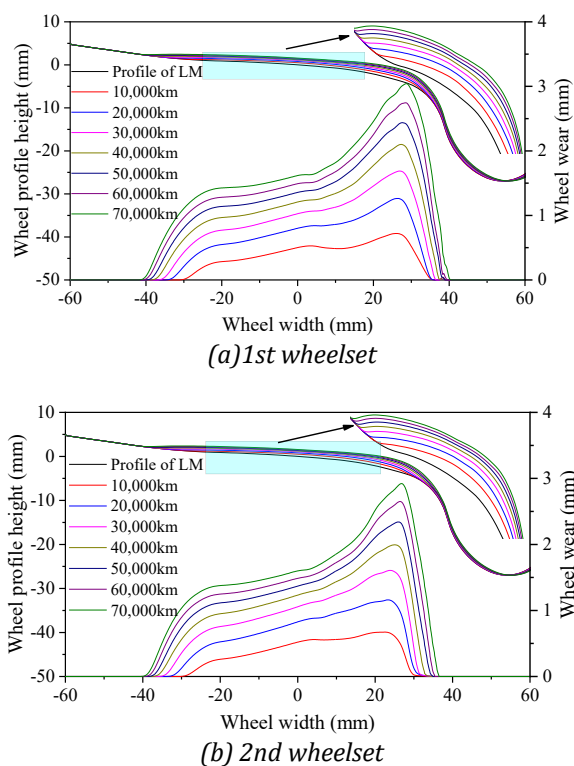


Figure 8: Wheel profile and wear variation

3.3 Wheel Wear Parameters

Figure 9 gives a schematic diagram of wheel wear parameters. The longitudinal variation at the 0 position of the nominal rolling circle is selected as the tread wear, which is called Tw; the transverse variation of 22 mm upward from the bottom of the flange is the flange wear, which is called Fw, and the wheel profile is divided into three main distribution areas. The root area of the wheel profile is near the flange side [20 ~ 70 mm]. The tread [-20 ~ 20 mm] is the midportion area of the wheel profile, which is the most concentrated area of wheel-rail contact. The tread [-70 ~ -20 mm] is the terminal area of the wheel profile.

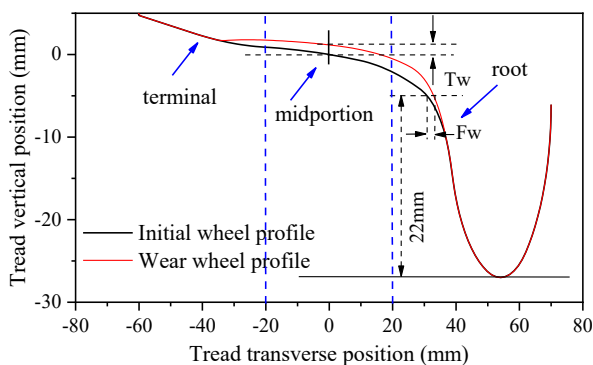


Figure 9: Wheel profile wear parameter diagram

Figure 10 shows the change of wheel tread and flange wear. There is little difference in tread wear between 1st and 2nd wheelsets. When the distance is between 10,000 and 60,000 km, the tread wear of 2nd wheelset is higher than that of 1st wheelset.

When the distance is between 10,000 and 50,000 km, the difference of tread wear is roughly normal distribution. When the distance is 30,000 km, the maximum difference is 0.032 mm. The increase of flange wear of 1st wheelset is very obvious, and the overall growth rate is higher than that of 2nd wheelset. The maximum growth rate is 1.930 mm at 20,000 ~ 70,000 km. The change range of 2nd wheelset is not large at 0 ~ 40,000 km, which is roughly stable. The maximum growth rate is 0.895 mm at 40,000 ~ 70,000 km. The difference of flange wear increases linearly with the running mileage, and the difference of flange wear increases the most at 20,000 ~ 40,000 km, from 0.207 mm to 1.004 mm. It can be seen from the above that under the running mileage of 70,000 km, the maximum wear of the 1st and 2nd wheelsets flange is 2.144 mm and 0.898 mm respectively, and the maximum flange wear difference is 1.246 mm.

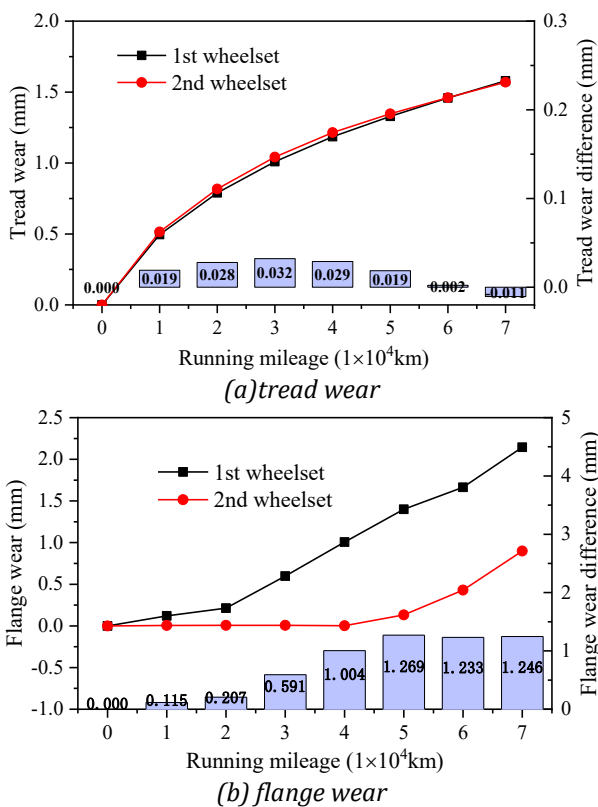


Figure 10: Variation of wheel wear parameters

4. Analysis of Wheel-Rail Contact Relationship

4.1 Wheel-Rail Contact Point Distribution

Table 2 shows the changes of wheel tread contact points under different mileages. When the initial LM wheel profile is matched with the CHN75 rail, the contact point of the wheel is in the area between [-35 ~ 40 mm], and the contact line is most concentrated in the position of [0 ~ 28 mm]. The distribution of the contact line at the position of [28 ~ 40 mm] on the flange side of the wheel profile is sparse. The rail

is mainly concentrated on the right side [11 ~ 35 mm] where the contact line is the most concentrated.

With the increase of running mileage, the contact lines of the 1st and 2nd wheelsets move to the end of the wheel, and the distribution range becomes wider. Among them, the contact lines of the 1st wheelset at the flange position [16 ~ 36 mm] are sparsely distributed at 10,000 ~ 30,000 km. Subsequently, there is no contact line at the wheel [16 ~ 38 mm] position under 50,000-70,000 km, while there is no contact line at the 2nd wheelset [15 ~ 35 mm] position under 60,000-70,000 km.

At this time, the wheel-rail contact point jump phenomenon may occur. The reason is that due to the serious wear of the wheel flange, the wheel tread at this position produces concave wear. Under 70,000 km, the wheel profile contact line is concentrated in the position of [- 40 ~ 20 mm], and the rail profile contact line is concentrated in the position of [- 14 ~ 14 mm].

Table 2. Change of wheel tread contact point

Operating mileage (10,000km)	1st wheelset	2nd wheelset
0		
1		
2		
3		
4		
5		
6		
7		

4.2 Equivalent Concicity

Figure 11 shows the change of equivalent concicity of different wheelsets. The equivalent concicity of the initial wheel profile increases significantly in the range of 3 ~ 7 mm, and the other positions tend to be stable. In the range of 0 ~ 10,000 km, the equivalent concicity of the 1st and 2nd wheelsets is higher than that of the initial profile in the range of 0 ~ 3 mm. With the increase of running mileage, the equivalent concicity value of 1st wheelset decreases, but it increases between 8 mm and 10 mm, and is

lower than the equivalent concicity of the initial profile as a whole. The overall 2nd wheelset will increase between 7 ~ 10 mm and is higher than the equivalent concicity of the initial wheel profile. From the change of the nominal equivalent concicity value, it can be seen that the 1st and 2nd wheelsets will increase in the early stage of operation, and decrease with the increase of the running mileage. The nominal equivalent concicity value of the 2nd wheelset is lower than that of the 1st wheelset.

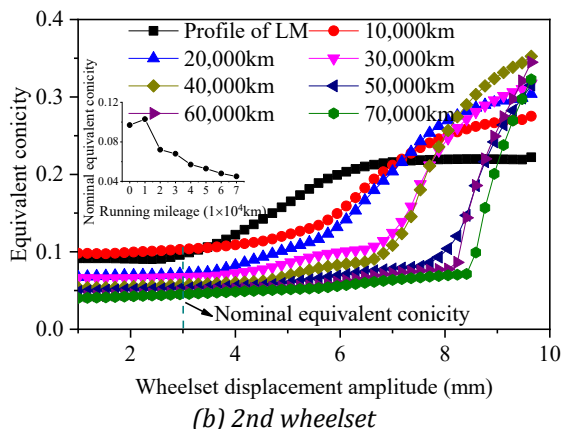
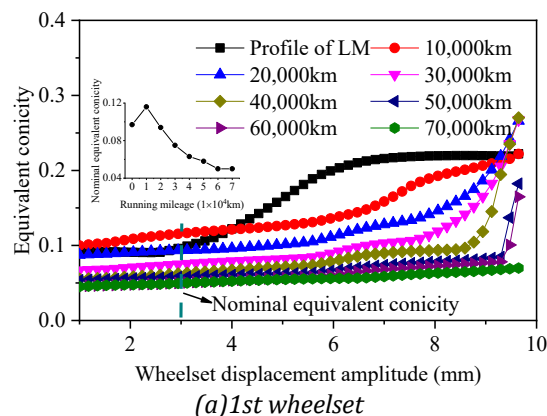


Figure 11: Change of equivalent concicity

4.3 Dynamic Wheel-Rail Contact Point

It can be seen from Figure 12 that when the heavy-haul freight wagon passes through the small radius curve, the centrifugal force of the car body will cause the outer wheel flange to contact with the rail most closely, resulting in the most serious wheel flange wear and rail side wear. The front bogie includes 1st and 2nd wheelset, which 1st wheelset contact the curve rail, and then the bogie returns the wheel-rail contact point to the initial position due to the swing of the car body. Based on the above line statistics, it can be seen that the wheel wear is the most serious when the freight wagon runs on a small radius curve of 500 m. Therefore, the dynamic change law of wheel-rail contact point on wheel tread when different wheel wear profiles are too small radius curves is explored. This index reflects the fluctuation of lateral range of wheel-rail contact.

The operating conditions are set as follows: the running speed of the freight wagon is 70 km / h, the radius of the curve is 500 m, the superelevation is 85

mm, the straight line is 30 m, the transition curve is 60 m, and the circular curve is 400 m, as shown in Figure 12.

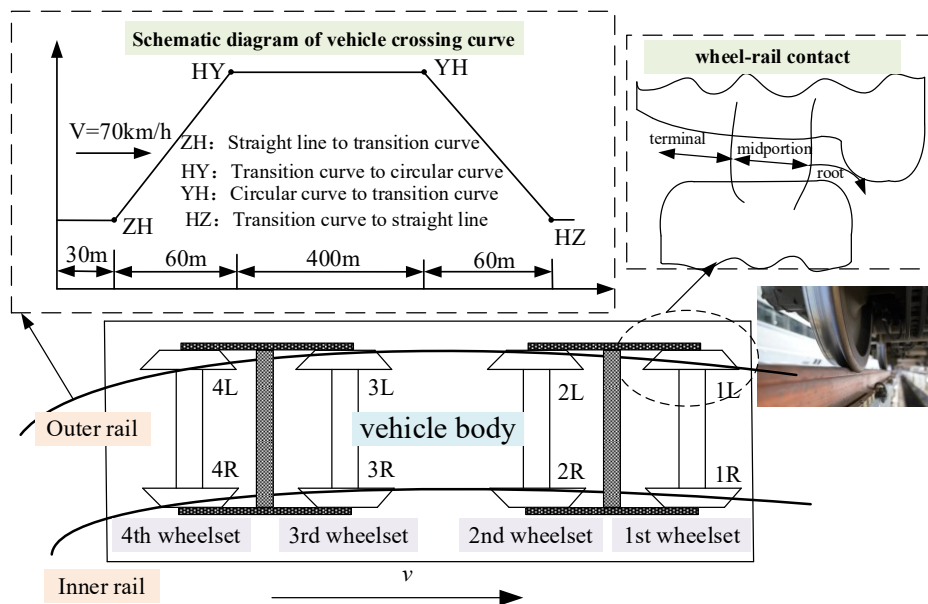
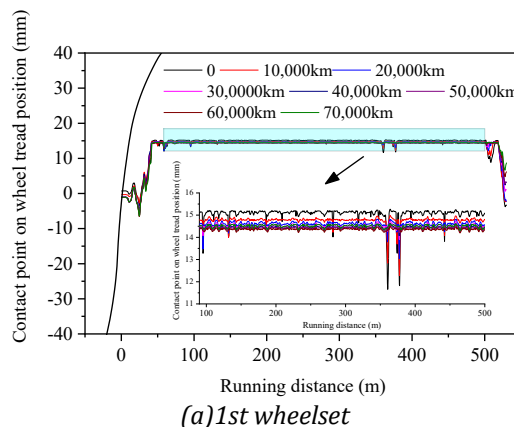


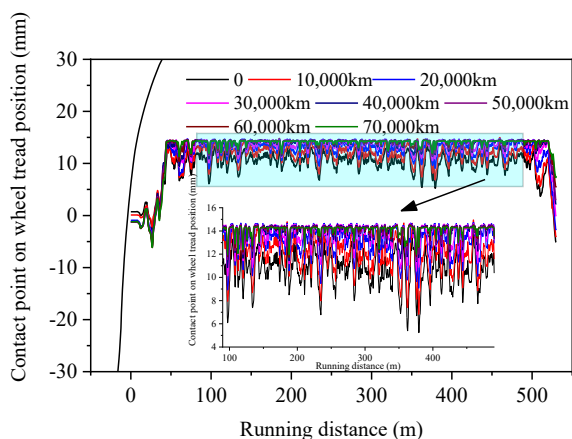
Figure 12: Vehicle passing curve and wheel-rail contact diagram

It can be seen from Figure 13 that when the vehicle passes the curve, the contact point of the outer wheel tread of the 1st and 2nd wheelsets is between the nominal rolling circle and the flange root. When the wheelset passes the ZH point, the contact point moves from the rolling circle position to the flange root. When the wheelset passes through the HY point, there is a phenomenon that the root of the flange contacts the rail, and the wheel-rail contact points fall on the flange. After the wheelset passes the YH point, with the increase of the running distance, the contact point slowly returns to the nominal rolling circle position from the root of the flange. On the circular curve, the contact point of the initial profile of the 1st wheelset fluctuates around 15.1 mm on the tread. With the increase of the running mileage, the contact point moves to the nominal rolling circle position. Among them, the contact point of wheel profile under 10,000 km fluctuates at 14.8 mm of wheel tread, and the contact point of wheel profile under 20,000 km fluctuates at 14.6 mm of wheel tread. Finally, with the increase of running mileage, the contact point of wheel profile fluctuates little, and the whole fluctuates at 14.3 mm. The contact point of the initial profile of the 2nd wheelset fluctuates greatly on the circular curve, and fluctuates at the position of the wheel profile [5.5 ~ 13.5 mm]. The contact point of the wheel profile under 10,000 km moves to the root of the flange, at the tread position [6.8 ~ 14.5 mm], and the contact point of the 20,000 km wheel profile is at the tread position [9.2 ~ 14.5 mm]. With the increase of

running mileage, the lower limit value of contact point moves to the flange position, and the upper limit value is stable at about 14.5 mm. The contact point of 70,000 km wheel profile fluctuates at the tread position [12 ~ 14.5 mm].

It can be seen from the above that the wheel profile wear rate is faster in the early stage of operation, and the 1st wheelset plays a guiding role when passing the curve. The contact point is close to the nominal rolling circle, and the wheel profile wear is serious. The wear of the wheel profile of the 2nd wheelset is smaller. With the increase of the running mileage, the contact point will move to the flange position, which is attributed to the bogie cross bar. The fluctuation of the contact point of the 2nd wheelset is greater than that of the 1st wheelset, and the wear of the vehicle profile is more uniform, while the wear of the 1st wheelset is more concentrated, which may produce concave wear.





(b) 2nd wheelset

Figure 13: The change of the position of the lateral contact point of the wheel tread when the vehicle passes through the small radius curve

5. Conclusions

In this paper, the vehicle-track coupling dynamic model is established based on UM software. The Kik-Piotrowski contact algorithm and Archard wear prediction model are used to simulate and predict wheel wear. The evolution law of wheel wear and the influence of worn wheel profile on wheel-rail contact relationship are analyzed, and the following conclusions are obtained.

(1) With the increase of running mileage, the wear width of the wheel increases. The 1st and 2nd wheelsets move about 10 mm to the terminal of the wheel, resulting in uniform wear at the tread [-40 ~ -30 mm] position, and move about 5 mm to the root of the wheel, resulting in serious wear of the wheel flange at the [30 ~ 35 mm] position, and wheel concave wear will occur. The wear rate of 1st and 2nd wheelsets flange is 0.306 mm / 10,000 km and 0.128 mm / 10,000 km.

(2) When the running mileage of the 1st and 2nd wheelsets reaches 50,000 km, the wheel-rail contact point will jump at the position of [15 ~ 38 mm], and the wheel will suffer serious concave wear. On the circular curve, with the increase of running mileage, the fluctuation range of the dynamic contact point of the 1st wheelset is more concentrated, while the fluctuation range of the 2nd wheelset is wider. Due to the cross bar of the bogie, the dynamic wheel-rail contact point of the 1st wheelset moves to the rolling circle position, and the dynamic wheel-rail contact point of the 2nd wheelset moves to the flange position.

(3) It is suggested that the wheel flange or rail side should be lubricated in the early stage of vehicle operation (0 ~ 40 000 km) to reduce the wear rate. When the wheel runs to 50,000 km, the contact point jump will occur at the root [16~38mm] of one wheel set, and the wheel should be repaired.

References

- [1] Deng Jiehang, Zhu Zitong, Li Hebi, et al. Study on Transportation Organization for 30 000-ton Heavy-haul Trains. *Railway Transport and Economy*, 2024, 46(03): 11-16. <https://doi.org/10.16668/j.cnki.issn.1003-1421.2024.03.02>.
- [2] Yan Quan Sun, Maksym Spiriyagin, Qing Wu, et al. Wheel-rail contact wear analysis on curved lubricated track for heavy haul locomotive studies. *Proceedings of the Institution of Mechanical Engineers, Part F: Journal of Rail and Rapid Transit*, 2024, 238: 967-976. <https://doi.org/10.1177/09544097241244411>.
- [3] Jun Lai, Yu Chen, Tao Liao, et al. Study on train running safety in railway switches and sharp curves considering wheel wear evolution. *Vehicle System Dynamics*, 2024: 1-25. <https://doi.org/10.1080/00423114.2024.2319277>.
- [4] Jian Mu, Jing Zeng, Qunsheng Wang, et al. Determination of mapping relation between wheel flat and wheel/rail contact force for railway freight wagon using dynamic simulation. *Proceedings of the Institution of Mechanical Engineers, Part F: Journal of Rail and Rapid Transit*, 2022, 236: 545-556. <https://doi.org/10.1177/09544097211030373>.
- [5] Pedro Henrique Alves Corrêa, Paola Gonzalez Ramos, Raidam Fernandes, et al. Effect of primary suspension and friction wedge maintenance parameters on safety and wear of heavy-haul rail vehicles. *Wear*, 2023, 524-525: 204748. <https://doi.org/10.1016/j.wear.2023.204748>.
- [6] Jury Auciello, Enrico Meli, Stefano Falomi, et al. Dynamic simulation of railway vehicles: wheel rail contact analysis. *Vehicle System Dynamics*, 2009, 47: 867-899. <http://dx.doi.org/10.1080/00423110802464624>.
- [7] Sajjad Z. Meymand, Alexander Keylin, Mehdi Ahmadian. A survey of wheel-rail contact models for rail vehicles. *Vehicle System Dynamics*, 2016, 54: 386-428. <http://dx.doi.org/10.1080/00423114.2015.1137956>.
- [8] Congcong Fang, Sulaiman A Jaafar, Wei Zhou, et al. Wheel-rail contact and friction models: A review of recent advances. *Proceedings of the Institution of Mechanical Engineers, Part F: Journal of Rail and Rapid Transit*, 2023, 237: 1245-1259. <https://doi.org/10.1177/09544097231156730>.
- [9] Luigi Romano, Michele Maglio, Stefano Bruni. Transient wheel-rail rolling contact theories. *Tribology International*, 2023, 186: 108600. <https://doi.org/10.1016/j.triboint.2023.108600>.

- [10] Filipe Marques,Hugo Magalhães,João Pombo, et al. A three-dimensional approach for contact detection between realistic wheel and rail surfaces for improved railway dynamic analysis, 2020: 1-34. <https://doi.org/10.1016/j.mechmachtheory.2020.103825>.
- [11] LI Hengli,LI Fu,WANG Xinrui, et al. Evolution of wheel wear and dynamics performance of heavy haul freight car. *Journal of Traffic and Transportation Engineering*, 2016, 16(05): 49-56.<https://doi.org/10.19818/j.cnki.1671-1637.2016.05.006>.
- [12] Oldrich Polach. Characteristic parameters of nonlinear wheel/rail contact geometry. *Vehicle System Dynamics*, 2010, 48: 19-36.<https://doi.org/10.1080/00423111003668203>.
- [13] Oldrich Polach,Dirk Nicklisch. Wheel/rail contact geometry parameters in regard to vehicle behaviour and their alteration with wear. *Wear*, 2016, 366-367: 200-208.<http://dx.doi.org/10.1016/j.wear.2016.03.029>.
- [14] [14] Binbin Liu,Stefano Bruni. Comparison of wheel-rail contact models in the context of multibody system simulation: Hertzian versus non-Hertzian. *Vehicle System Dynamics*, 2022, 60: 1076-1096.<https://doi.org/10.1080/00423114.2020.1847297>.
- [15] Binbin Liu,Edwin Vollebregt,Stefano Bruni. Review of conformal wheel/rail contact modelling approach-es: towards the application in rail vehicle dynamics simulation. *Vehicle System Dynamics*, 2024, 62: 1355-1379.<https://doi.org/10.1080/00423114.2023.228438>.
- [16] Nico Burgelman,Matin Sh. Sichani,Roger Enblom, et al. Influence of wheel-rail contact modelling on vehicle dynamic simulation. *Vehicle System Dynamics*, 2015, 53: 1190-1203.<http://dx.doi.org/10.1080/00423114.2015.1039550>.
- [17] Chaojiang Hao,Jingmang Xu,Yao Qian, et al. Impact of wheel profile evolution on the lateral motion characteristics of a high-speed vehicle navigating through turnout. *Vehicle System Dynamics*, 2024, 62: 2079-2097.<https://doi.org/10.1080/00423114.2023.274468>.
- [18] Jingmang Xu,Ping Wang,Li Wang, et al. Effects of profile wear on wheel-rail contact conditions and dynamic interaction of vehicle and turnout. *Advances in Mechanical Engineering*, 2016, 8: 1-14. <http://dx.doi.org/10.1177/1687814015623696>
- [19] Elisa Butini,Lorenzo Marini,Martina Meacci, et al. An innovative model for the prediction of wheel - Rail wear and rolling contact fatigue. *Wear*, 2019, 436-437: 203025.<https://doi.org/10.1016/j.wear.2019.203025>.
- [20] Peng Wang,Xiaoxuan Yang,Gongquan Tao, et al. Development of a wheel wear prediction model considering the interaction of abrasive block-wheel and wheel-rail. *Wear*, 2024, 550: 205418.<https://doi.org/10.1016/j.wear.2024.205418>.
- [21] Ying Jin,Makoto Ishida,Akira Namura. Experimental simulation and prediction of wear of wheel flange and rail gauge corner. *Wear*, 2011, 271: 259-267.<http://dx.doi.org/10.1016/j.wear.2010.10.032>.
- [22] Gengzhuo Miao,Ren Luo,Huailong Shi. Wheel wear prediction for high-speed trains by considering wheel-rail elastic deformation. *Proceedings of the Institution of Mechanical Engineers, Part F: Journal of Rail and Rapid Transit*, 2024, 238: 921-930.<https://doi.org/10.1177/09544097241239089>.
- [23] Kaiser I,Poll G,Vinolas J. Modelling the impact of structural flexibility of wheelsets and rails on the wheel-rail contact and the wear. *Wear*, 2020, 203(20): 445-476. <https://doi.org/10.1016/j.wear.2020.203445>.
- [24] Sudhir Kumar Singh,Amit Kumar Das,Sanjay R. Singh, et al. Prediction of rail-wheel contact parameters for a metro coach using machine learning. *Expert Systems with Applications*, 2023, 215: 119343.<https://doi.org/10.1016/j.eswa.2022.119343>.
- A. Shebani,S. Iwnicki. Prediction of wheel and rail wear under different contact conditions using artificial neural networks. *Wear*, 2018, 406-407: 173-184. <https://doi.org/10.1016/j.wear.2018.01.007>.
- [25] A.C. Pires,G.R. Mendes,G.F.M. Santos, et al. Indirect identification of wheel rail contact forces of an instrumented heavy haul railway vehicle using machine learning. *Mechanical Systems and Signal Processing*, 2021, 160: 107806.<https://doi.org/10.1016/j.ymssp.2021.107806>.
- [26] Gao Ennan,Tao Gongquan,Ren Dexiang, et al. Multi-objective optimization of a metro wheel profile to reduce wheel flange wear and RCF considering the distribution density of wheel-rail contact points. *Vehicle System Dynamics*, 2024: 1-16. <https://doi.org/10.1080/00423114.2024.2342532>.
- [27] Molatefi H,Mazraeh A,Shadfar M, et al. Advances in Iran railway wheel wear management A practical approach for selection of wheel profile using numerical methods and comprehensive field tests. *Wear*, 2019, 424-425(5-6): 97-110. <https://doi.org/10.1016/j.wear.2019.02.016>.
- [28] Pacheco P A D P,Endlich C S,Vieira K L S, et al. Optimization of heavy haul railway wheel profile

- based on rolling contact fatigue and wear performance. *Wear*, 2023, 522: 204704. <https://doi.org/10.1016/j.wear.2023.204704>.
- [29] Liu Pengfei,Liu Hongjun,Gao Hao, et al. Elastic Vibration of Wheelset and Its Dynamic Effect on Railway Heavy-Haul Freight Wagon. *Journal of Southwest Jiaotong University*, 2021, 57(01): 1-9.<https://doi.org/10.3969/j.issn.0258-2724.20210024>.
- [30] Liu Pengfei,Wang Kaiyun,Zhai Wanming, et al. Investigation of wheel-rail contact geometry and dynamic matching for heavy haul freight wagon with 30t axle load. *Journal of Chongqing University of Technology(Natural Science)*, 2013, 27(09): 22-26. [https://doi.org/10.3969/j.issn.1674-8425\(z\).2013.09.005](https://doi.org/10.3969/j.issn.1674-8425(z).2013.09.005).
- [31] Zhai Wanming. *Vehicle-track coupled dynamics*. Beijing: Science Press, 2015. <https://doi.org/10.1080/00423110802621561>.
- [32] Hao Kai,Liu Pengfei,Wang Chen, et al. Influence of curve proportion weight on wheel wear of heavy haul locomotive. *Journal of Beijing Jiaotong University*, 2023, 47(04): 171-178.<https://doi.org/10.11860/j.issn.1673-0291.20220168>.
- [33] Liu Pengfei,Hao Kai,Wang Chen, et al. Study on Wheel Profile Evolution for Dynamic Curve Passing Performance of Heavy Haul Locomotive. *Machinery Design & Manufacture*, 2023(12): 24-29.<https://doi.org/10.19356/j.cnki.1001-3997.20230209.023>.
- [34] Wang Pu,Wang Shuguo. Numerical Prediction of Wheel Wear Development of Heavy-haul Freight Car Under Complex Operation Conditions. *Journal of Tongji University(Natural Science)*, 2019, 47(01): 71-78. <https://doi.org/CNKI:SUN:TJZ.0.2019-01-009>.
- [35] Liu Pengfei,Wei Kai,Wang Kaiyun, et al. Testing of modified primary stiffness for heavy-haul locomotives operating on sharper radius curves. *Proceedings of the Institution of Mechanical Engineers Part K Journal of Multi-body Dynamics*, 2019, 233(3): 531-548. <https://doi.org/10.1177/1464419319836006>.
- [36] Yuyi Li,Zunsong Ren,Roger Enblom, et al. Wheel wear prediction on a high-speed train in China. *Vehicle System Dynamics*, 2020, 58: 1839-1858.<https://doi.org/10.1080/00423114.2019.1650941>.
- [37] Archard JF. Contact and rubbing of flat surfaces. *Journal of Applied Physics*, 1953, 24(8): 981-988.
- [38] K. Six,A. Meierhofer,G. Müller, et al. Physical processes in wheel-rail contact and its implications on vehicle-track interaction. *Vehicle System Dynamics*, 2015, 53: 635-650.<http://dx.doi.org/10.1080/00423114.2014.983675>.
- [39] Ulf Olofssona,Yi Zhua,Saeed Abbasia, et al. Tribology of the wheel-rail contact aspects of wear, particle emission and adhesion. *Vehicle System Dynamics*, 2013: 1-30.
- [40] Zhikun Song,Linjun Guo,Xiaoyi Hu, et al. Research on causes and countermeasures of wheel polygon wear based on Kik-Piotrowski contact model. *Vehicle System Dynamics*, 2024, 62: 955-975.<https://doi.org/10.1080/00423114.2023.2203866>.
- [41] Piotrowski J,Kik W. A simplified model of wheel/rail contact mechanics for non-Hertzian problems and its application in rail vehicle dynamic simulations. *Vehicle System Dynamics*, 2008, 46(1-2): 27-48. <https://doi.org/10.1080/00423110701586444>.